

Electric-field control of spin transitions in molecular compounds

O. I. Utesov^{1,2,3}, S. Burdin⁴, P. Rosa⁵, M. Gonidec⁵, L. Poggini⁵, and S. V. Andreev^{6,*}

¹National Research Center “Kurchatov Institute” B.P. Konstantinov Petersburg Nuclear Physics Institute, Gatchina 188300, Russia

²St. Petersburg State University, 7/9 Universitetskaya nab., St. Petersburg 199034, Russia

³Nanotechnology Research and Education Centre of the Russian Academy of Sciences, St. Petersburg Academic University, 194021 St. Petersburg, Russia

⁴University of Bordeaux, LOMA UMR-CNRS 5798, F-33405 Talence Cedex, France

⁵CNRS, Univ. Bordeaux, Bordeaux INP, ICMCB, UMR 5026, F-33600 Pessac, France

⁶ITMO University, Saint-Petersburg 197101, Russia

 (Received 20 October 2019; revised manuscript received 30 November 2019; published 18 December 2019)

We present a theoretical model of spin transitions in stacks of molecular layers. Our model captures the already established physics of these systems (thermal hysteretic transitions and crossovers) and suggests a way towards *in situ* control of this physics by means of an external electric field. Our results pave the way toward both temperature and voltage controllable organic memory.

DOI: [10.1103/PhysRevB.100.235126](https://doi.org/10.1103/PhysRevB.100.235126)

I. INTRODUCTION

Spin crossover molecular compounds (SCO) have been intensively discussed during the past decades in connection with data recording and sensing [1,2]. These systems switch between a low- (LS) and a high-spin (HS) state as the temperature is increased. In some cases the conversion has a hysteretic behavior characterized by heating and cooling characteristic temperatures, T_c^\uparrow and T_c^\downarrow , respectively. These temperatures can be easily made on the order of the room temperature. By applying temporary heating (e.g., a laser pulse) one can switch an initially LS state to a HS state. The latter will be preserved until cooling the device below the operational temperature.

At the microscopic level, the conversion is due to switching between two electronic states of molecules characterized by different occupation of e_g and t_{2g} subsets of $3d$ metal orbitals. The LS state arises from the closed-shell (t_{2g}^6) and the HS state from the open-shell ($t_{2g}^4 e_g^2$) configurations [1]. These differ by magnetic, optical, and structural properties and can be altered by pressure, temperature and light irradiation [3–7] which makes SCO promising for new functional materials.

SCO complexes consist of transition metal ions surrounded by organic ligands. One may play with the SCO thermodynamics by carefully designing the ligands. At the spin crossover, the enthalpy remains essentially constant with temperature and the SCO phenomenon is driven by entropy. For the HS state the electronic contribution to entropy is higher than that of the LS state. As the SCO needs to be accompanied by a structural change of the complex resulting in weaker bonds in the HS state, the vibrational contribution to entropy for the latter is also higher than for the LS state. This situation leads to a thermal conversion from the LS state to HS state upon increasing temperature [8,9].

A comprehensive theoretical description of the SCO physics, as demonstrated in numerous works [10–18], can be

done in terms of the Ising-like model:

$$\hat{H} = \Delta \sum_{i=1}^N \hat{S}_z^i - J \sum_{i,j} \hat{S}_z^i \hat{S}_z^j, \quad (1)$$

with the relevant parameters being the energy splittings between the LS and HS states 2Δ , and the coupling constant $J > 0$ describing the interaction between the nearest neighbors (“cooperativity effect”). Due to degeneracy of the open-shell $t_{2g}^4 e_g^2$ electronic configuration the HS state has larger statistical weight and thus stabilizes at sufficiently large temperatures.

The situation is less understood for thin films of SCO molecules. The studies of SCO films with thicknesses ranging from 5 to 1000 nm conclude that the thermally driven spin transition in such systems is similar to that of the bulk [8,19–27]. However, when the thickness is decreased down to submonolayer or a few monolayers in coverage, the SCO behavior seems to be modified by the interaction with the substrate [28–35]. In particular, some of us have recently demonstrated that a thick film of $[\text{Fe}(\text{H}_2\text{B}(\text{pz})_2)_2(\text{bipy})]$ deposited by thermal sublimation on an organic ferroelectric substrate maintains the SCO behavior [36], whereas for thinner films (under 15 nm) the SCO behavior was controlled by the substrate polarization [36–38].

On the general grounds, one may expect the substrate to modify the splitting Δ between the spin states of the molecules. First, the splittings of molecules which constitute the boundary layer are clearly affected by microscopic Van-der-Waals interaction with the surface of the substrate. This effect seems to be responsible for the recent experimental observations [34,36,37]. Second, macroscopic electric field \mathbf{E} produced by the ferroelectric substrate should modify the splittings in all layers according to the formula

$$\Delta(\mathbf{E}) = \Delta_0 + \frac{1}{2} \sum_{\alpha,\beta=x,y,z} v_{\alpha\beta} E_\alpha E_\beta, \quad (2)$$

*Serguey.Andreev@gmail.com

where we assume the field being uniform over the sample, Δ_0 is the bare splitting at $E = 0$ and $\nu_{\alpha\beta}$ is some phenomenological *symmetric* tensor to be defined from the experiment. Existence of the coupling of type (2) may be argued as follows. Due to the electrostriction the electric field would modify the pressure P acting on the system (or, alternatively, the system volume V). The change in the pressure P can be written as

$$\delta P = \frac{1}{2} \sum_{\alpha,\beta} \left[\frac{\partial(\alpha_{\alpha\beta} V)}{\partial V} \right]_T E_\alpha E_\beta, \quad (3)$$

where $\alpha_{\alpha\beta}$ is the polarizability of the sample [39]. This change of the pressure, on the other hand, would modify the spin splittings due to an inverse ‘‘magnetostriction’’ effect,

$$\Delta = \Delta_0 + \left(\frac{\partial \Delta}{\partial P} \right)_{\delta P=0} \delta P. \quad (4)$$

What we call ‘‘magnetostriction’’ in the context of the model (1) is a phenomenological way to account for the fact that the average metal-ligand bond length is longer in the HS state than in the LS state [40,41]. For instance, the characteristic temperature of the crossover $T_{1/2}$ was shown to grow linearly with the pressure [42,43]. As we shall see, this experimental fact justifies the assumption (4) *a posteriori* and, therefore, supports the existence of the relation (2). It is also worth it to point out that a relation of type (2) has previously been obtained by microscopic considerations assuming dipolar coupling of SCO complexes to the electric field [44]. The calculated variation of $T_{1/2}$ in the applied electric field was in qualitative agreement with the experiment.

Implementation of the coupling (2) would build a bridge between the field of spin transition polymers and ferroelectricity and pave a way toward both temperature- and voltage-controllable organic memory. A crucial first step on this way is a theoretical analysis of implication of the hypothesis of a tunable Δ on the physics of spin transitions as described by the Hamiltonian (1). This analysis is presented in our paper. We start by formulating the theoretical model we use in the present study. In Sec. II, under certain assumptions, we obtain the effective Hamiltonian of the system in the form (1). For the bulk problem its mean-field solution is given in Sec. III. The already established physics of thermal spin transitions and crossovers is presented in Sec. III A. The main result of this subsection is the existence of the critical value of the ratio Δ/J above which the first-order thermal transition (hysteresis) turns to a smooth crossover. We obtain a simple analytical expression for this ratio and confirm it by numerics. In Sec. III B we show that isothermal variation of Δ can also lead to a hysteresis. Arguments, analogous to those presented in Sec. III A, when applied to the spin transition induced by variation of Δ , yield the maximum and minimum temperatures at which the hysteresis under an electric field would be possible.

In Sec. IV we turn to the discussion of layered systems. We show that, for sufficiently weak coupling between the layers, it should be possible to observe a staircase in the fraction of molecules in the HS state γ_{HS} as a function of Δ . We discuss such *multistability* in terms of a phase diagram of Δ versus the ratio of inter- to intralayer couplings for two layers. For

sufficiently large interlayer coupling the transition occurs in both layers simultaneously. This switching can be performed either as in bulk (by varying either temperature or Δ) or by variation of the energy splitting Δ only in the boundary layer (due to, e.g., interaction with the surface of the substrate). This result of our theoretical model holds qualitatively for few layers (thin films). In contrast, in films with a large number of layers, variation of Δ in the boundary layer has no impact on γ_{HS} . The situation here is similar to the bulk, in agreement with the experiment [36,37].

II. THEORETICAL MODEL AND METHODS

Our starting point is the following phenomenological Hamiltonian

$$\hat{H} = \sum_i \hat{H}_i + \sum_{i,j} \hat{V}_{ij} \quad (5)$$

where

$$\hat{H}_i = E_0^i |0\rangle_i \langle 0|_i + E_1^i \sum_{\alpha=1..g} |1_\alpha\rangle_i \langle 1_\alpha|_i \quad (6)$$

and

$$\hat{V}_{ij} = \sum_{\sigma_1, \sigma_2, \sigma_3, \sigma_4} J_{\sigma_1, \sigma_2, \sigma_3, \sigma_4, i, j} |\sigma_1\rangle_i \otimes |\sigma_2\rangle_j \langle \sigma_3|_j \otimes \langle \sigma_4|_i. \quad (7)$$

The Hamiltonian (5) is a general model of an assembly of two-level systems with interaction. We attribute $|0\rangle_i$ to the low-spin (LS) and $|1_\alpha\rangle_i$ to the one of the g -fold degenerate high-spin (HS) states of the i th molecule, respectively. By introducing the pseudospin operators

$$\begin{aligned} \hat{S}_z &= \sum_\alpha |1_\alpha\rangle \langle 1_\alpha| - |0\rangle \langle 0|, \\ \hat{S}_+ &= \hat{S}_x + i\hat{S}_y = \sum_\alpha |1_\alpha\rangle \langle 0|, \\ \hat{S}_- &= \hat{S}_x - i\hat{S}_y = \sum_\alpha |0\rangle \langle 1_\alpha|, \end{aligned} \quad (8)$$

we rewrite the Hamiltonian (5) in the useful form

$$\hat{H} = \sum_i \Delta_i \hat{S}_z^i - \sum_{i,j} \sum_{\mu, \nu=(+, -z)} \hat{S}_\mu^i M_{\mu\nu} \hat{S}_\nu^j \quad (9)$$

where we have introduced $\Delta_i = (E_1^i - E_0^i)/2$ for the molecular energy splitting. The crucial assumption now is to take the second term in (9) in the block form $\hat{V}_{ij} = -(M_{zz} \hat{S}_z^i \hat{S}_z^j + M_{+-} \hat{S}_+^i \hat{S}_-^j + M_{-+} \hat{S}_-^i \hat{S}_+^j)$ and assume the interaction between the nearest neighbors only. The problem is thus projected onto an effective Heisenberg XXZ model. The first term in the above equation describes the static interaction between the spins, whereas inclusion of the second term would allow us to study the dynamical response to perturbations. In this work we shall examine the case $M_{zz} = J > 0$ (ferromagneticlike coupling) and use the static mean-field approximation $\langle \hat{S}_z^i \rangle = m$ and $\langle \hat{S}_\pm^i \rangle = 0$. Thus, the model is reduced to an effective Ising model (1) with ‘‘magnetic field’’ Δ .

To take into account the structure of the system (the layers are arranged on the top of each other along the growth direction) we shall further introduce J_\parallel for the interlayer coupling and J_\perp to describe interaction between the layers. The

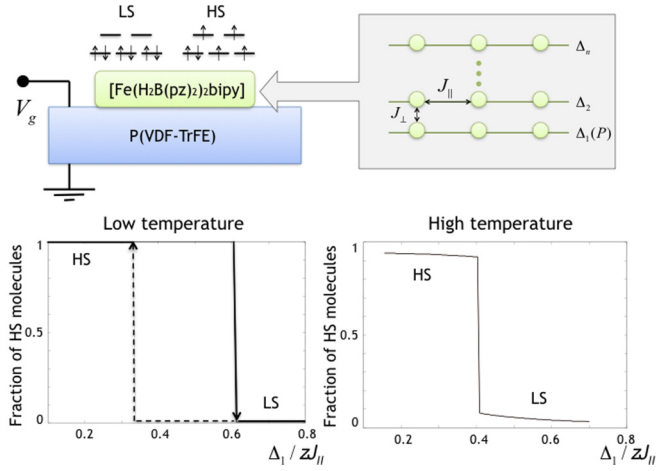


FIG. 1. Switching of the spin state of a stack of n molecular thin films $[\text{Fe}(\text{H}_2\text{B}(\text{pz})_2)\text{bipy}]$ (green rectangle) by the polarization of a ferroelectric substrate (blue rectangle). Each molecule can be in two possible states, “low spin” (LS) and “high spin” (HS) characterized by zero and nonzero spin projection on the growth axis, respectively. To describe the behavior of the system we use the model shown in the gray rectangle on the right (see the text). In the bottom panel we show the fraction of HS molecules γ as a function of the HS/LS splitting at the boundary layer calculated for two different temperatures T . At low T one has a first order transition (hysteresis) which turns to a crossover at high T . We used the model (32) with $n = 2$, $\sigma = 0.5$ and the following set of parameters: (i) $t = 0.5$, $\delta_2 = 0.2$ and (ii) $t = 1$, $\delta_2 = 1$.

quantities z_{\perp} and z_{\parallel} will be the corresponding coordination numbers (see Fig. 1).

After the model Hamiltonian has been constructed, all the relevant thermodynamic quantities can be obtained starting from the partition function

$$Z = \text{Tr}(e^{-\beta \hat{H}}), \quad (10)$$

where $\beta = 1/k_B T$ is the inverse temperature of the system. The free energy reads

$$F = -k_B T \ln(Z) \quad (11)$$

and, considered as a function of the average magnetization m , can be used to describe transitions between different states, as we show below.

III. SINGLE LAYER

It is instructive to discuss first the simplest case of a homogeneous single-layer system (which, in the frame of our model, is equivalent to the bulk). The diagram in Fig. 2 shows possible ways to switch between the spin states. Below we explain and discuss this scheme in more detail.

A. Thermal hysteresis

The Hamiltonian of the system reads

$$\hat{H}_1 = \Delta \sum_{i=1}^N \hat{S}_z^i - \sum_{i,j} J \hat{S}_z^i \hat{S}_z^j, \quad (12)$$

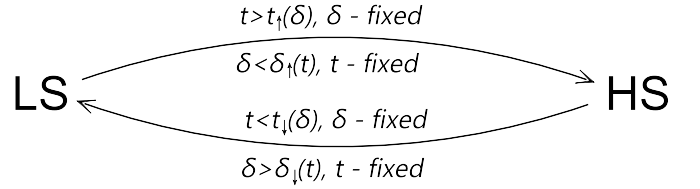


FIG. 2. Ways to switch the spin state of the system. In a certain range of parameters (see the main text) the transitions are characterized by hysteresis and can be accomplished by varying either the temperature or the energy splitting between the LS and HS states.

where the summation in the second term is over the nearest neighbors and N is the total number of molecules in the layer. By introducing the coordination number z (the number of the nearest neighbors) and using the mean-field approximation we rewrite the above Hamiltonian in the form

$$\hat{H}_1 = \sum_{i=1}^N (\Delta - J_z m) \hat{S}_z^i + \frac{1}{2} \sum_{i=1}^N J_z m^2, \quad (13)$$

where $J_z m$ is an effective Weiss field. The “magnetization” m is related to the fraction γ_{HS} of the HS molecules by

$$\gamma_{\text{HS}} = \frac{m+1}{2}. \quad (14)$$

Using Eq. (10), we calculate the free energy

$$\frac{F}{N} = \frac{J_z m^2}{2} - k_B T \ln[ge^{-(\Delta - J_z m)/k_B T} + e^{(\Delta - J_z m)/k_B T}]. \quad (15)$$

Here g is the degeneracy of the HS state, discussed above.

It is convenient to introduce the dimensionless parameters $t = k_B T / J_z$ and $\delta = \Delta / J_z$. The dimensionless free energy per molecule then reads

$$f(m) = \frac{m^2}{2} - t \ln[ge^{-(\delta - m)/t} + e^{(\delta - m)/t}]. \quad (16)$$

Considered as a function of m the free energy can have either two minima separated by a barrier or one minimum. The latter situation is always realized at sufficiently large temperatures t . At moderate temperatures there can be two physically distinct scenarios depending on the value of δ : first order transition with hysteresis and a crossover.

In order to describe these two scenarios analytically we first consider the low-temperature limit $t \ll 1$ and $\delta \sim t$, where simple analytical expressions can be derived. Their region of validity will be discussed below. Near the $m = 1$ point one can neglect the second exponent in the logarithm in Eq. (16) and obtain the following form for the free energy:

$$f(m) = \frac{m^2}{2} - m - t \ln g + \delta, \quad (17)$$

which evidently yields a local minimum $m = 1$. Analogously, near $m = -1$,

$$f(m) = \frac{m^2}{2} + m - \delta, \quad (18)$$

and there is a local minimum at $m = -1$. There is also a maximum at $m \approx 0$. So, the properties of the system are

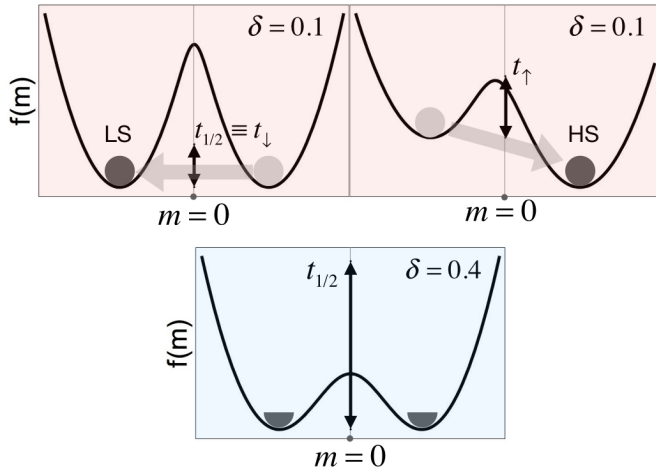


FIG. 3. Free energy profiles at the characteristic temperatures t_{\uparrow} , t_{\downarrow} in the hysteresis (upper panel) and $t_{1/2}$ in the crossover (lower panel) regimes distinguished by the values of δ (see also Fig. 4). Black double arrows indicate the temperature scale to be compared with the height of the potential barrier separating the two minima.

defined by three free energies

$$\begin{aligned} f(+1) &\approx -1/2 - t \ln g + \delta, \\ f(-1) &\approx -1/2 - \delta, \\ f(0) &= -t \ln (ge^{-\delta/t} + e^{\delta/t}). \end{aligned} \quad (19)$$

Obviously, at very low temperature the system will be in the LS state. From the condition $f(+1) = f(-1)$ we can determine the temperature at which the ground state becomes doubly degenerate (we denote it $t_{1/2}$ since in the crossover regime at this temperature one has $\gamma = 1/2$). Simple calculation yields

$$t_{1/2} = \frac{2\delta}{\ln g}. \quad (20)$$

This obtained formula is consistent with the well-known expression $T_{1/2} = \Delta H/\Delta S$, where ΔH is the enthalpy and ΔS is the entropy of the spin conversion [1,45].

Two cases should be distinguished. The barrier height $h(t)$ at the temperature $t_{1/2}$ can either exceed or be lower than this temperature. In the first case (upper panel of Fig. 3) the thermal fluctuations at $t = t_{1/2}$ are insufficient to induce a transition from LS to HS state. One has to attain some larger temperature t_{\uparrow} at which $h(t_{\uparrow}) = t_{\uparrow}$ in order to observe the transition. On the other hand, when decreasing t , an inverse transition from HS to LS state apparently cannot take place at t_{\uparrow} , so that one should define some t_{\downarrow} such that $t_{\downarrow} < t_{\uparrow}$, and a natural way to do it is to let $t_{\downarrow} \equiv t_{1/2}$. In this case one may speak about a first-order like transition featuring hysteresis. Using equations above we can find the critical value δ_c which separates the two different regimes:

$$h(t_{1/2}) = f(0) - f(-1)|_{t=t_{1/2}} = t_{1/2}, \quad (21)$$

which solution gives

$$\delta_c = \frac{\ln g}{4(1 + \ln 2)}. \quad (22)$$

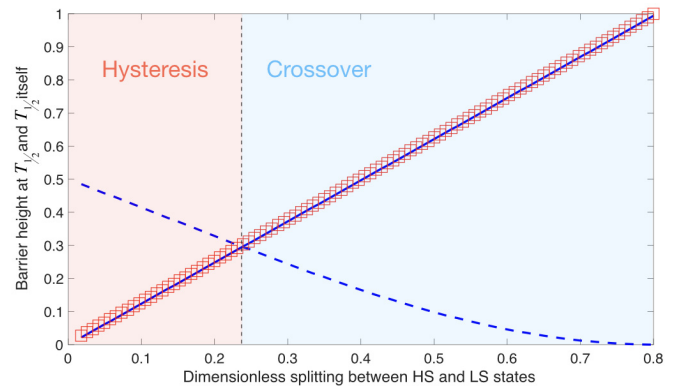


FIG. 4. Dependence of the barrier height $h(t_{1/2})$ (dashed line) and the characteristic temperature $t_{1/2}$ (open squares and solid line) on the parameter δ . The critical value $\delta = 0.24$ is defined as a point at which $h(t_{1/2}) = t_{1/2}$. For $\delta < 0.24$ one has a regime of hysteresis (left area, see the text). For $\delta > 0.24$ there is a smooth crossover between LS and HS states and vice versa along the same curve. For the $t_{1/2}$ dependence the open squares are used for the numerical result, whereas the solid line is the analytic expression (20). Note an excellent agreement between the two.

For numerical estimates we take $g = 5$, which corresponds to the e_g/t_{2g} splitting in the octahedral symmetry. One should bear in mind, however, that this value may be modified when taking into account molecular vibrations [18] and structural disorder [46]. We find $\delta_c \approx 0.24$. For $\delta < 0.24$ the barrier height $h(t_{1/2}) > t_{1/2}$ and one has a first order thermal spin transition characterized by a hysteresis loop. Indeed, after simple calculations one can derive the equation for t_{\uparrow} :

$$\delta = -\frac{t_{\uparrow}}{2} \ln \left[\frac{e^{\frac{1}{2t_{\uparrow}} - 1} - 1}{g} \right], \quad (23)$$

which yields $t_{\uparrow} > t_{1/2}$ at $\delta < \delta_c$. We check the formulas (20), (22), and (23) numerically and find that they hold with excellent accuracy in the whole range of the relevant values of $\delta \lesssim \delta_c$.

For $\delta > \delta_c$ the situation is very different. Now one has $h(t_{1/2}) < t_{1/2}$ (lower panel of Fig. 3), which means that the first order transition is replaced by a smooth crossover from LS to HS and vice versa along the same curve. The two distinct regimes are shown on the left ($\delta < 0.24$) and right ($\delta > 0.24$) sides of Fig. 4.

At $\delta \approx 0.75$ the barrier at $t = t_{1/2} \approx 0.93$ disappears, which means that the potential relief almost flattens and the two minima of $f(m)$ merge. Below, we will use the value $t_{1/2} = 0.93$ to quantify the situation where in the equation

$$m = \tanh \frac{m}{t_{1/2}}, \quad (24)$$

[which is the exact equation for extrema of the free energy (16) at $t_{1/2}$ (20)] the distinct roots at $m \approx \pm 1$ disappear.

To close this subsection we notice that the obtained linear growth of $t_{1/2}$ with δ corroborates *a posteriori* the assumption (4) of the linear dependence of Δ on the pressure. Indeed, linear growth of $T_{1/2}$ with the applied pressure has been previously reported in the experimental studies [42,43].

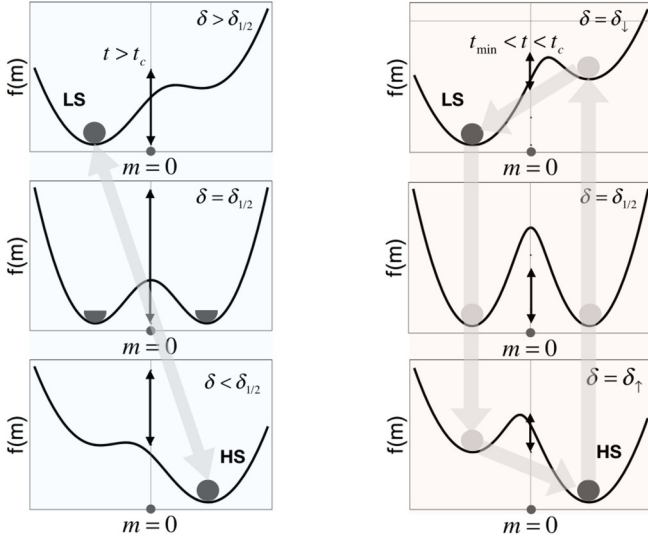


FIG. 5. Evolution of the free energy landscape in the course of isothermal crossover (on the left) and hysteresis (on the right) induced by variation of the energy splitting δ . Black double arrows indicate the temperature scale to be compared with the height of the potential barrier separating the two minima. Note that this temperature is fixed for each column comprising three graphs. However, the scale on each graph has been adjusted to better present the free energy profile, so the length of the arrows has been adjusted accordingly.

B. Isothermal switching

The above analysis may be put another way by fixing the temperature and considering variations of the parameter δ around

$$\delta_{1/2} \equiv \frac{t \ln g}{2}. \quad (25)$$

Here, again, the subscript 1/2 signifies an equal distribution of the molecules over the spin states in the crossover regime. The crossover occurs at high temperatures falling onto the right side of the diagram in Fig. 4 (previously classified as the thermal crossover region) and is characterized by smooth transition from the LS to the HS state as one *decreases* δ . This is sketched on the left side of Fig. 5.

At low temperatures one has an *isothermal* hysteresis. This is illustrated on the right side of Fig. 5. Here, two well-defined characteristic values of δ exist, which we denote δ_{\uparrow} and δ_{\downarrow} . The point $\delta = \delta_{\uparrow}$ corresponds to the situation where the global minimum of the free energy is the HS state and the thermal fluctuations (characterized by the magnitude of t) are sufficiently strong to jump into this state from the LS minimum. The point $\delta = \delta_{\downarrow}$ corresponds to the transition from the HS to the LS state. By using Eqs. (20) and (23) one may obtain

$$\delta_{\uparrow} - \delta_{1/2} = -\frac{\delta_{1/2}}{\ln g} \ln [e^{\ln g / 4\delta_{1/2} - 1} - 1] \quad (26)$$

and

$$\delta_{\downarrow} - \delta_{1/2} = \frac{\delta_{1/2}}{\ln g} \ln [e^{\ln g / 4\delta_{1/2} - 1} - 1]. \quad (27)$$

By requiring $\delta_{\uparrow} > 0$, one obtains

$$\delta_{1/2} > \frac{\ln g}{4[\ln(g+1)+1]} \approx 0.14. \quad (28)$$

Using Eq. (25) it can be rewritten as the following restriction on the temperature:

$$t > t_{\min} = \frac{1}{2[\ln(g+1)+1]} \approx 0.18. \quad (29)$$

At lower temperatures even at $\delta = 0$ the barrier remains too high for the transition from the LS to HS state could take place. In general, the higher the temperature, the smaller variation of δ around $\delta_{1/2}$ is required to perform the switching.

The isothermal hysteresis and crossover regimes are separated by the point

$$t_c = \frac{2\delta_c}{\ln g} \approx 0.29, \quad (30)$$

where δ_c is given by (22). The low-temperature region where the hysteresis takes place is defined by $t_{\min} < t < t_c$. The upper bound is consistent with the requirement $\delta_{\downarrow} > \delta_{1/2}$.

To summarize, in the temperature window specified above we find a hysteretic behavior controlled by the energy splitting between LS and HS state. The splitting, in turn, may be controlled by the boundary strains and by the macroscopic electric field produced by the substrate as we have argued in the Introduction. Noteworthy, existence of the minimal temperature t_{\min} may explain the unidirectional character of the transition observed in micrometric samples [44]: At $t < t_{\min}$ only a transition from the HS state to the LS state is possible by increasing δ . A full hysteresis cycle could possibly be realized at higher temperatures (but less than t_c). However, for the studied samples this would require stronger coupling to the electric field (to perform switching from the HS to the LS state).

IV. MULTILAYER PROBLEM. MULTISTABILITY

After having established the fundamentals of the thermal hysteresis/crossover in bulk, we now turn to an investigation of a layered structure deposited on a ferroelectric substrate. As we have conjectured in the Introduction, the substrate primarily affects the value of the molecular energy splitting Δ_1 at the boundary layer. In the frame of our model such coupling can be described by Eq. (4), where the pressure P is due to boundary effects (e.g., the epitaxial strain [34] or the thermal expansion mismatch). Clearly, such boundary strains are also affected by the electric polarization due to piezodeformation of the substrate. However, in contrast to the bulk problem, existence of the relation of type (3) here is not granted. We therefore merely assume a possibility of tuning Δ_1 , leaving the detailed investigation of the underlying mechanisms for future studies. Increasing the ratio

$$\sigma = \frac{J_{\perp}}{z_{\parallel} J_{\parallel}}, \quad (31)$$

drives the system to a cooperative regime, where the change in Δ_1 results in switching of the spin state of the whole sample (simultaneous transition from LS to HS in both layers). To

develop a feel of the effect it is instructive to consider first the case of two layers.

A. Two layers

The dimensionless free energy of the double-layer system reads

$$f(m_1, m_2) = \frac{1}{2}(m_1^2 + m_2^2 + 2\sigma m_1 m_2) - t[\ln(ge^{-e_1/t} + e^{e_1/t}) + \ln(ge^{-e_2/t} + e^{e_2/t})], \quad (32)$$

where

$$e_{1,2} = \delta_{1,2} - m_{1,2} - \sigma m_{2,1} \quad (33)$$

and $g = 5$ accounts for the fivefold degeneracy of the HS state. We have introduced the following notations: $f = F/NJ_{\parallel}z_{\parallel}$, N being the number of molecules in one layer, $t = k_B T/J_{\parallel}z_{\parallel}$, $\delta_{\alpha} = \Delta_{\alpha}/J_{\parallel}z_{\parallel}$.

We start from the similar to the previous section analysis of the free energy at low temperatures. We shall refer to states with different m_1 and m_2 as (m_1, m_2) .

Near $(+1, +1)$ point we have the free energy in the form

$$f \approx \frac{m_1^2 + m_2^2 + 2\sigma m_1 m_2}{2} - (1 + \sigma)(m_1 + m_2) - 2t \ln g + (\delta_1 + \delta_2). \quad (34)$$

This function evidently has minimum at $(+1, +1)$. The same analysis can be also performed for $(-1, -1)$, $(-1, +1)$, and $(+1, -1)$ points. It shows that $(-1, -1)$ is a local minimum. However, two other points $(-1, +1)$ and $(+1, -1)$ can be minima only if $\sigma < \sigma_c < 1$, where σ_c is dependent on t , δ_1 , δ_2 and will be determined below. Corresponding free energies read

$$f(-1, -1) \approx -1 - \sigma - (\delta_1 + \delta_2), \quad (35)$$

$$f(+1, +1) \approx -1 - \sigma - 2t \ln g + (\delta_1 + \delta_2). \quad (36)$$

At $\sigma < \sigma_c$ we have additional minima with free energy

$$f(+1, -1) \approx \sigma - 1 - t \ln g + \delta_1 - \delta_2, \quad (37)$$

$$f(-1, +1) \approx \sigma - 1 - t \ln g + \delta_2 - \delta_1. \quad (38)$$

These additional minima make the transition from the LS in both layers $(-1, -1)$ to HS $(+1, +1)$ indirect, for example sequence $(-1, -1) \rightarrow (+1, -1) \rightarrow (+1, +1)$ can arise. We shall refer to this case as *multistability*.

It is seen from the equations above that at low temperatures $(-1, -1)$ state is the global minimum. At

$$t_c^{(2)} = \frac{\delta_1 + \delta_2}{\ln g} \quad (39)$$

we have $f(+1, +1) = f(-1, -1)$, thus it is the temperature when the ground state is doubly degenerate.

We also notice a possibility for $(+1, -1)$ or $(-1, +1)$ to be a global minimum in some temperature interval of temperatures near $t_c^{(2)}$. Indeed, one can see from Eqs. (35) and (37) that if $2\sigma < \delta_1 - \delta_2$ then $f(-1, +1) < f(-1, -1)$ at $t_c^{(2)}$.

At high enough interlayer interaction ($\sigma > \sigma_c$) the transition from LS to HS occurs simultaneously in both layers. In this case the minima at $(+1, -1)$ and $(-1, +1)$ disappear in the critical temperature $t_c^{(2)}$ vicinity. In order to quantify σ_c we rewrite (32) using new variables, $m_I = m_1 + \sigma m_2$ and $m_{II} = m_2 + \sigma m_1$. We obtain the free energy in the form

$$f(m_1, m_2) = \frac{m_I^2 + m_{II}^2 - 2\sigma m_I m_{II}}{2(1 - \sigma^2)} - t[\ln(ge^{(m_I - \delta_1)/t} + e^{(\delta_1 - m_I)/t}) + \ln(ge^{(m_{II} - \delta_2)/t} + e^{(\delta_2 - m_{II})/t})]. \quad (40)$$

In a special case of $\delta_1 = \delta_2$ at $t_c^{(2)}$ the system of equations which defines free energy minima reads [cf. Eq. (24)]

$$\frac{m_I - \sigma m_{II}}{1 - \sigma^2} = \tanh(m_I/t_c^{(2)}),$$

$$\frac{m_{II} - \sigma m_I}{1 - \sigma^2} = \tanh(m_{II}/t_c^{(2)}). \quad (41)$$

At small enough $t_c^{(2)}$ all the right hand sides of these equations can be substituted by ± 1 and the system gives previously discussed solutions, but written in new variables: $(-1 - \sigma, -1 - \sigma)$, $(1 + \sigma, 1 + \sigma)$, $(1 - \sigma, \sigma - 1)$, and $(\sigma - 1, 1 - \sigma)$. From Eq. (24) we saw that if the tanh argument becomes small enough (≈ 1) the potential relief near the minimum flattens. Here the tanh argument is multiplied either by $1 + \sigma$ or by $1 - \sigma$. Thus, the minima for LS and HS in both layers are much more stable, and the minima with opposite spin states can be destroyed by large enough σ . Corresponding equation reads

$$\frac{1 - \sigma_c}{t_c^{(2)}} \approx 1 \Leftrightarrow \sigma_c \approx 1 - \frac{2\delta}{\ln g}. \quad (42)$$

It is also applicable if $(\delta_1 - \delta_2)/(\delta_1 + \delta_2) \ll 1$.

At $\sigma > \sigma_c$ barrier height at $t_c^{(2)}$ is defined with good accuracy by $f(+1, -1) - f(-1, -1)$ or $f(-1, +1) - f(-1, -1)$. It gives $h = 2\sigma - (\delta_2 - \delta_1)$ or $h = 2\sigma - (\delta_1 - \delta_2)$, correspondingly. At $\delta_1 = \delta_2$ the minimal barrier height is $2\sigma_c \approx 2 - 2t_c^{(2)}$. Thus, at $t_c^{(2)} < 2/3$ the first order transition takes place. At $t_c^{(2)} > 2/3$ the character of the transition depends on σ . As in the one-layer problem, by variation of δ in both layers the system can be switched from LS to HS state and vice versa.

However, we notice a new feature with respect to the one-layer problem. One can tune the splitting δ_1 at one layer, due to the interaction with the substrate, keeping the splitting at the other one δ_2 and the temperature t fixed. This idea is illustrated in Fig. 6, where the phase diagram of the system in (σ, t) plane is mapped onto the corresponding phase diagram in the (σ, δ_1) plane. Variation of δ_1 around

$$\delta_{1,c} = t \ln g - \delta_2 \quad (43)$$

allows one to switch from LS to HS and vice versa simultaneously in both layers, i.e., to induce a spin transition in one layer by its interaction with another layer.

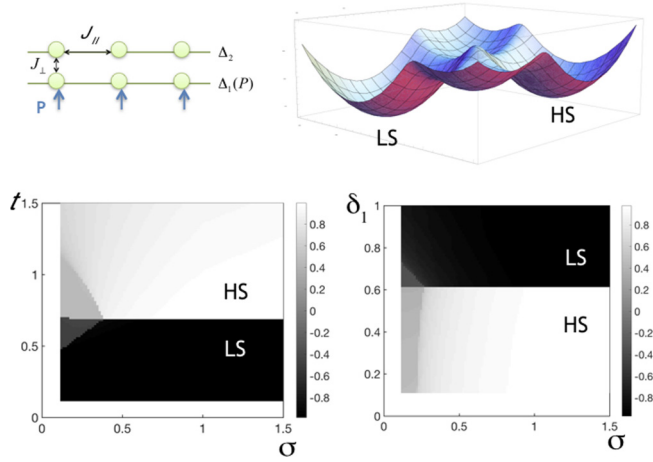


FIG. 6. (Top) Schematic illustration of a two-layer setting and the corresponding free energy landscape $f(m_1, m_2)$. The labels LS and HS denote the areas in the (m_1, m_2) plane where the entire system is in the low-/high-spin states, respectively. (Bottom) (σ, t) (left, $\delta_1 = 0.1$) and (σ, δ_1) (right, $t = 1$) phase diagrams of a double-layer system. We take $\delta_2 = 1$. The color is the average magnetization $m = (m_1 + m_2)/2$: black corresponds to $m = -1$ and white to $m = +1$. For sufficiently large σ one can switch the spin state of the whole system by varying δ_1 near some critical value δ_{1c} .

B. Multiple layers

Let us now consider some general results for n layers. The free energy in this case has the form:

$$\begin{aligned}
 f(m_1, \dots, m_n) &= \frac{1}{2}(m_1^2 + \dots + m_n^2 + 2\sigma m_1 m_2 \\
 &+ 2\sigma m_2 m_3 + \dots + 2\sigma m_{n-1} m_n) \\
 &- t[\ln(g e^{(m_1 + \sigma m_2 - \delta_1)/t}) + e^{(\delta_1 - m_1 - \sigma m_2)/t}) \\
 &+ \ln(g e^{(m_2 + \sigma(m_1 + m_3) - \delta_2)/t}) + e^{(\delta_2 - m_2 - \sigma(m_1 + m_3))/t}) + \dots \\
 &+ \ln(g e^{(m_{n-1} + \sigma(m_{n-2} + m_n) - \delta_{n-1})/t}) \\
 &+ e^{(\delta_{n-1} - m_{n-1} - \sigma(m_{n-2} + m_n)/t}) \\
 &+ \ln(g e^{(m_n + \sigma m_{n-1} - \delta_n)/t}) + e^{(\delta_n - m_n - \sigma m_{n-1})/t})]. \quad (44)
 \end{aligned}$$

Similar to previous section calculations give minima at $(+1, \dots, +1)$ and $(-1, \dots, -1)$ with free energies

$$f(-1, \dots, -1) \approx -n/2 - (n-1)\sigma - n\bar{\delta}, \quad (45)$$

$$f(+1, \dots, +1) \approx -n/2 - (n-1)\sigma - nt \ln g + n\bar{\delta}, \quad (46)$$

where $\bar{\delta} = (\delta_1 + \dots + \delta_n)/n$ is the mean value of δ_α . From these equations we get

$$t_c^{(n)} = \frac{2\bar{\delta}}{\ln g}. \quad (47)$$

Conditions of other possible minima stability [they have the form $(\pm 1, \dots, \pm 1)$] at $t_c^{(n)}$ are similar to those discussed

above. They depend on the value of arguments in tanh functions:

$$\tanh \frac{m_1 + \sigma m_2}{t_c^{(n)}}, \quad (48)$$

$$\tanh \frac{m_i + \sigma(m_{i-1} + m_{i+1})}{t_c^{(n)}}, \quad (49)$$

$$\tanh \frac{m_n + \sigma m_{n-1}}{t_c^{(n)}}. \quad (50)$$

Let's start from $(-1, \dots, -1)$ state. If we flip some layer in the middle we will have condition of this texture stability in the form $(1 - 2\sigma)/t_c^{(n)} > 1$. However textures with $(-1, \dots, -1, +1, \dots, +1)$ —“domain walls”—are much more stable, the corresponding condition reads $1/t_c^{(n)} > 1$. Thus, we can estimate the barrier height at $t_c^{(n)}$ as $f(-1, \dots, -1, +1, \dots, +1) - f(-1, -1, \dots, -1)$. For the $(-1, \dots, -1, +1, \dots, +1)$ state the potential relief for layers at the “domain wall” are almost flat at $1/t_c^{(n)} > 1$ and the average spin of the corresponding layers is zero. So, we obtain for equal δ_i case:

$$\begin{aligned}
 f(-1, \dots, -1, +1, \dots, +1) \\
 \approx -\frac{n-2}{2} - (n-2)\delta - (n-3)\sigma - \frac{4\delta}{\ln g} (\ln 2\sqrt{g}). \quad (51)
 \end{aligned}$$

Thus, the barrier height reads

$$h \approx 1 + 2\sigma - 2t_c^{(n)} \ln 2. \quad (52)$$

This quantity can be used for estimating whether we have the first order transition or smooth crossover.

As in Sec. IV A we notice a possibility of switching the spin state of the whole system by variation of δ_1 . However, it is seen from Eq. (47) that the impact of δ_1 has an additional factor $2/n$ in comparison with (39), which makes it rather weak for $n \gg 1$. Thus, the interaction of the first layer with the substrate, which is important in the double-layer problem, is almost negligible. So, similar to the one-layer problem, the spin state of the whole sample can be switched by the temperature or by the δ variation in all the layers, by means of, e.g., external electric field. An important issue, which should be taken into account is the existence of the domain walls, which are metastable at low temperatures.

V. SUMMARY AND CONCLUSION

To conclude, we theoretically address the problem of spin transitions in the systems consisting of molecular layers. In the framework of the mean-field approach we obtain the already established physics of this systems, which includes the first-order-like thermal phase transitions with hysteresis and smooth crossovers from the low spin state of the system to the high spin state. We further consider the possibility of isothermal switching by means of an electric field, which is provided by, e.g., ferroelectric substrate. For the bulk problem (single layer) we determine the conditions under which the hysteresis due to the variation of the energy splitting between

the LS and HS states can appear. Experimental observation of such hysteresis would be a crucial step toward technological implementation of SCO films in nanoelectronics.

In the case of layered structures we find that two qualitatively different situations should be distinguished: the system consisting of few layers ($n \sim 1$) and multilayer systems with $n \gg 1$. In both cases it should be possible to observe a staircase in γ_{HS} as a function of the electric field in a certain range of parameters. We call such phenomenon *multistability*. For $n \sim 1$, provided the interlayer coupling is sufficiently large, all the layers can be switched simultaneously by switching only the first layer by, e.g., microscopic interaction with the surface of the substrate. We believe this effect to be relevant to the experimental findings [36,37]. In contrast, multilayer systems with $n \gg 1$ behave analogously to the bulk: The boundary plays no role and the spin state of the film can be controlled

either by temperature or by the macroscopic electric field produced by the substrate. The latter must be sufficiently strong for the coupling (2) could come into play. One should also take care of highly stable intermediate states—“domain walls”—which should be avoided in the switching process. Detailed investigation of this phenomenon is beyond the scope of this paper and will be given elsewhere.

ACKNOWLEDGMENTS

S.V. thanks A. Cano for helpful discussions and acknowledges the financial supports by CNRS and by Russian Science Foundation (Grant No. 18-72-00013). Contribution to the work by O.I.U. was funded by RFBR according to the research Project No. 18-02-00706.

-
- [1] O. Kahn, J. Krober, and C. Jay, *Adv. Mater.* **4**, 718 (1992).
- [2] G. Felix, W. Nicolazzi, M. Mikolasek, G. Molnár, and A. Bousseksou, *Phys. Chem. Chem. Phys.* **16**, 7358 (2014).
- [3] P. Gutlich and H. A. Goodwin, *Spin Crossover in Transition Metal Compounds III* (Springer-Verlag, Berlin, Heidelberg, 2004), Vol. 235.
- [4] M. A. Halcrow, *Spin-Crossover Materials: Properties and Applications* (John Wiley and Sons Ltd, Oxford, 2013).
- [5] A. Bousseksou, G. Molnár, L. Salmon, and W. Nicolazzi, *Chem. Soc. Rev.* **40**, 3313 (2011).
- [6] P. Gutlich, A. Hauser, and H. Spiering, *Angew. Chem., Int. Ed. Engl.* **33**, 2024 (1994).
- [7] K. Boukheddaden and A. Bailly-Reyre, *Europhys. Lett.* **103**, 26005 (2013).
- [8] C. Lefter, V. Davesne, L. Salmon, G. Molnar, P. Demont, A. Rotaru, and A. Bousseksou, *Magnetochemistry* **2**, 18 (2016).
- [9] D. Chernyshov, H.-B. Bürgi, M. Hostettler, and K. W. Törnroos, *Phys. Rev. B* **70**, 094116 (2004).
- [10] A. B. Koudryavtsev and W. Linert, *J. Struct. Chem.* **50**, 1181 (2009).
- [11] A. B. Koudriavtsev and W. Linert, *J. Struct. Chem.* **51**, 335 (2010).
- [12] A. B. Koudriavtsev and W. Linert, *Monatsh. Chem.* **141**, 601 (2010).
- [13] J. Wajnflasz, *Phys. Status Solidi B* **40**, 537 (1970).
- [14] R. A. Bari and J. Sivadrière, *Phys. Rev. B* **5**, 4466 (1972).
- [15] V. Zelentsov, G. Lapushkin, S. Sobolev, and V. Shipilov, *Dokl. Akad. Nauk SSSR* **289**, 393 (1986).
- [16] A. Bousseksou, J. Nasser, J. Linares, K. Boukheddaden, and F. Varret, *J. Phys. I (France)* **2**, 1381 (1992).
- [17] J. Linares, I. Sahbani, F. Desvoix, P. Dahoo, and K. Boukheddaden, *J. Phys.: Conf. Ser.* **1141**, 012073 (2018).
- [18] A. Bousseksou, H. Constant-Machado, and F. Varret, *J. Phys. I* **5**, 747 (1995).
- [19] K. Senthil Kumar, Y. Bayeh, T. Gebretsadik, F. Elemo, M. Gebrezgiabher, M. Thomas, and M. Ruben, *Dalton Trans.* **48**, 15321 (2019).
- [20] H. Naggert, A. Bannwarth, S. Chemnitz, T. von Hofe, E. Quandt, and F. Tuczek, *Dalton Trans.* **40**, 6364 (2011).
- [21] S. Shi, G. Schmerber, J. Arabski, J.-B. Beaufrand, D. Kim, S. Boukari, M. Bowen, N. Kemp, N. Viart, G. Rogez *et al.*, *Appl. Phys. Lett.* **95**, 043303 (2009).
- [22] T. Palamarcu, J. C. Oberg, F. El Hallak, C. F. Hirjibehedin, M. Serri, S. Heutz, J.-F. Létard, and P. Rosa, *J. Mater. Chem.* **22**, 9690 (2012).
- [23] M. Gruber, T. Miyamachi, V. Davesne, M. Bowen, S. Boukari, W. Wulfhekel, M. Alouani, and E. Beaupaire, *J. Chem. Phys.* **146**, 092312 (2017).
- [24] T. Mahfoud, G. Molnár, S. Cobo, L. Salmon, C. Thibault, C. Vieu, P. Demont, and A. Bousseksou, *Appl. Phys. Lett.* **99**, 053307 (2011).
- [25] N. Baadji, M. Piacenza, T. Tugsuz, F. Della Sala, G. Maruccio, and S. Sanvito, *Nat. Mater.* **8**, 813 (2009).
- [26] M. Atzori, L. Poggini, L. Squillantini, B. Cortigiani, M. Gonidec, P. Bencok, R. Sessoli, and M. Mannini, *J. Mater. Chem. C* **6**, 8885 (2018).
- [27] L. Poggini, M. Milek, G. Londi, A. Naim, G. Poneti, L. Squillantini, A. Magnani, F. Totti, P. Rosa, M. M. Khusniyarov *et al.*, *Materials Horizons* **5**, 506 (2018).
- [28] T. G. Gopakumar, F. Matino, H. Naggert, A. Bannwarth, F. Tuczek, and R. Berndt, *Angew. Chem., Int. Ed.* **51**, 6262 (2012).
- [29] T. G. Gopakumar, M. Bernien, H. Naggert, F. Matino, C. F. Hermanns, A. Bannwarth, S. Mühlenberend, A. Krüger, D. Krüger, F. Nickel *et al.*, *Chem. Eur. J.* **19**, 15702 (2013).
- [30] A. Pronschinske, Y. Chen, G. F. Lewis, D. A. Shultz, A. Calzolari, M. Buongiorno Nardelli, and D. B. Dougherty, *Nano Lett.* **13**, 1429 (2013).
- [31] M. Bernien, H. Naggert, L. M. Arruda, L. Kipgen, F. Nickel, J. Miguel, C. F. Hermanns, A. Krüger, D. Krüger, E. Schierle *et al.*, *ACS nano* **9**, 8960 (2015).
- [32] B. Warner, J. C. Oberg, T. G. Gill, F. El Hallak, C. F. Hirjibehedin, M. Serri, S. Heutz, M.-A. Arrio, P. Sainctavit, M. Mannini *et al.*, *J. Phys. Chem. Lett.* **4**, 1546 (2013).
- [33] L. Poggini, G. Londi, M. Milek, A. Naïm, P. Chen, V. Lanzilotto, B. Cortigiani, F. Bondino, E. Magnano, E. Otero, P. Sainctavit, M.-A. Arrio, A. Juhin, M. Marchivie, M. Khusniyarov, F. Totti, P. Rosa, and M. Mannini, *Nanoscale* **11**, 20006 (2019).

- [34] C. Fourmantal, S. Mondal, R. Banerjee, A. Bellec, Y. Garreau, A. Coati, C. Chacon, Y. Girard, J. Lagoute, S. Rousset *et al.*, *J. Phys. Chem. Lett.* **10**, 4103 (2019).
- [35] T. Delgado, C. Enachescu, A. Tissot, L. Guénée, A. Hauser, and C. Besnard, *Phys. Chem. Chem. Phys.* **20**, 12493 (2018).
- [36] X. Zhang, T. Palamarciuc, J.-F. Létard, P. Rosa, E. V. Lozada, F. Torres, L. G. Rosa, B. Doudin, and P. A. Dowben, *Chem. Commun.* **50**, 2255 (2014).
- [37] X. Zhang, T. Palamarciuc, P. Rosa, J.-F. Létard, B. Doudin, Z. Zhang, J. Wang, and P. A. Dowben, *J. Phys. Chem. C* **116**, 23291 (2012).
- [38] C. Wäckerlin, F. Donati, A. Singha, R. Baltic, S. Decurtins, S.-X. Liu, S. Rusponi, and J. Dreiser, *J. Phys. Chem. C* **122**, 8202 (2018).
- [39] L. D. Landau and E. M. Lifshitz, *Electrodynamics of Continuous Media, rev. and enl.*, edited by E. M. Lifshitz and L. P. Pitaevskii (Pergamon Press, Oxford, 1984).
- [40] B. Gallois, J. A. Real, C. Hauw, and J. Zarembowitch, *Inorg. Chem.* **29**, 1152 (1990).
- [41] H. Spiering, K. Boukheddaden, J. Linares, and F. Varret, *Phys. Rev. B* **70**, 184106 (2004).
- [42] P. Á. Szilágyi, S. Dorbes, G. Molnár, J. A. Real, Z. Homonnay, C. Faulmann, and A. Bousseksou, *J. Phys. Chem. Solids* **69**, 2681 (2008).
- [43] P. Guionneau and E. Collet, in *SpinCrossover Materials: Properties and Applications*, edited by M. A. Halcrow (John Wiley & Sons, Ltd., Hoboken, NJ, 2013), pp. 507–526.
- [44] C. Lefter, R. Tan, J. Dugay, S. Tricard, G. Molnár, L. Salmon, J. Carrey, W. Nicolazzi, A. Rotaru, and A. Bousseksou, *Chem. Phys. Lett.* **644**, 138 (2016).
- [45] H. Bolvin, *Chem. Phys.* **211**, 101 (1996).
- [46] D. Chernyshov, N. Klinduhov, K. W. Törnroos, M. Hostettler, B. Vangdal, and H.-B. Bürgi, *Phys. Rev. B* **76**, 014406 (2007).